



Engineering of a bio-functionalized hybrid off-the-shelf heart valve



Svenja Hinderer^{a,b,c}, Jan Seifert^d, Miriam Votteler^a, Nian Shen^b, Johannes Rheinlaender^d, Tilman E. Schäffer^d, Katja Schenke-Layland^{a,b,e,*}

^aUniversity Women's Hospital, Eberhard-Karls-University Tübingen, 72076 Tübingen, Germany

^bDept. of Cell and Tissue Engineering, Fraunhofer Institute for Interfacial Engineering and Biotechnology (IGB), 70569 Stuttgart, Germany

^cInstitute for Interfacial Process Engineering and Plasma Technology (IGVP), University of Stuttgart, 70569 Stuttgart, Germany

^dInstitute of Applied Physics and LISA+, Eberhard-Karls-University Tübingen, 72076 Tübingen, Germany

^eDept. of Medicine/Cardiology, Cardiovascular Research Laboratories, David Geffen School of Medicine at UCLA, Los Angeles, CA, USA

ARTICLE INFO

Article history:

Received 1 October 2013

Accepted 31 October 2013

Available online 13 December 2013

Keywords:

ECM (extracellular matrix)

Non-woven fabric

Nanotopography

Cardiac tissue engineering

Mechanical properties

ABSTRACT

Currently available heart valve replacements are limited in long-term performance or fail due to leaflet thickening, lack of growth or remodeling potential. In order to address these issues, it is necessary to mimic multiple factors of the native valvular extracellular matrix (ECM) such as architecture, mechanical behavior and biochemical signals. Here, we successfully generated an electrospun PEGdma–PLA scaffold adapted to the structure and mechanical properties of native valve leaflets. Valvular interstitial cells (VICs) and valvular endothelial cells (VECs) were seeded on the scaffold and when cultured under physiological conditions in a bioreactor, the construct performed like a native leaflet. Atomic force microscopy (AFM) was employed to obtain detailed mechanical information from the leaflets, which enabled the first layer-specific measurement of the Young's modulus. Interestingly, spongiosa stiffness was much lower compared to the fibrosa and ventricularis. Moreover, investigations into human fetal heart valve development identified collagen type I and versican as important structural proteins. As a proof of principle, these proteins were introduced to the scaffold, demonstrating the ability to bio-functionalize the hybrid valve based on nature's blueprint.

© 2013 The Authors. Published by Elsevier Ltd. Open access under [CC BY-NC-ND license](http://creativecommons.org/licenses/by-nc-nd/3.0/).

1. Introduction

A major limitation of the currently clinically available heart valve replacements is their incapability to grow or remodel post-implantation [1]. The valvular extracellular matrix (ECM) is a complex fibrous network composed of structural proteins such as collagens, elastic fibers and microfibrils as well as signaling molecules like water-storing proteoglycans (PGs), glycosaminoglycans (GAGs) and growth factors [2]. Electrospinning is a suitable method to generate fibrous scaffolds that mimic the ECM structure [3–5]. A high electric field is applied to a droplet polymer fluid. As the force from the electric field overcomes the surface tension of the polymer droplet solution, a fiber is formed, which travels in spinning

motions to the counter electrode, while the solvent evaporates [3]. By changing parameters, for example polymer, solvent, voltage or electrode distance, the fiber size as well as the mechanical properties of the scaffold can be adjusted [6]. Additionally, it is possible to electrospin ECM components in order to biochemically functionalize the material [5]. It has been previously shown that the presence of defined signaling molecules, three-dimensionality and appropriate mechanical properties significantly impact cell survival, adhesion, migration, proliferation and differentiation [7–10]. In natural ECM, the Young's modulus strongly varies depending on the organ. Bone tissue for example has a stiffness of 10^6 – 10^7 kPa, meanwhile skin is much more elastic with a modulus of 10–100 kPa [7]. The matrix density and thus the stiffness of a matrix can be used as a cue for stem cell fate decision [8]. Accordingly, mesenchymal stem cells were differentiated into neural tissue when cultured on hydrogels with a stiffness of 0.1 kPa, into myogenic tissue when exposed to 11 kPa hydrogels and osteogenic differentiation was achieved when the cells were cultured on 34 kPa matrices [8]. Maturation of neonatal rat cardiomyocytes was realized exposing the cells to 10 kPa, which was defined as the stiffness of native rat myocardium [11]. The Young's modulus is an important parameter for tissue growth and remodeling. Therefore,

* Corresponding author. Fraunhofer IGB Stuttgart, Department of Cell and Tissue Engineering, Nobelstr. 12, 70569 Stuttgart, Germany. Tel.: +49 711 970 4082; fax: +49 711 970 4158.

E-mail addresses: katja.schenke-layland@igb.fraunhofer.de, ksl@igb.fraunhofer.de (K. Schenke-Layland).

it is important to identify the mechanical properties of the intact tissue and translate these findings to organ- and tissue-tailored biomaterials design [12].

Heart valve leaflets are permanently exposed to a high pressure of 120/80 mmHg as well as to laminar and oscillatory shear stress due to blood flow [13]. An engineered heart valve material should therefore not only mimic the mechanical properties of the native ECM, but also withstand the mechanical forces in vivo. In addition to comprehensive materials and cell–matrix interaction analyses, we employed atomic force microscopy (AFM) in order to measure the Young's modulus in each layer of native heart valve leaflets. Here, we aimed to design a hybrid bio-functionalized heart valve that mimics the native aortic valve, which can be potentially manufactured as off-the-shelf medical product.

2. Materials and methods

The studies involving human tissues were in accordance with institutional guidelines and were approved by the local Ethics Committees at the University of California Los Angeles (UCLA) and the University Hospital of the Eberhard Karls University (UKT) (UCLA IRB #05-10-093; UKT IRB #356/2008B02 and #406/2011B01). The research was carried out in compliance with the rules for investigation of human subjects, as defined in the declaration of Helsinki.

2.1. Electrospun scaffold fabrication

Electrospinning was performed using a customized electrospinning device as described before [5]. Equal amounts of poly(ethylene glycol) dimethacrylate (PEGdma; 687529, Sigma, Steinheim, Germany) and poly(L-lactide) (PLA; 93578, Sigma) were dissolved in 1,1,1,3,3,3 hexafluoro-2-propanol (HFP; 804515, Merck, Darmstadt, Germany). One percent 2-hydroxy-4'-(2-hydroxyethoxy)-2-methylpropiophenone (Initiator; 410896, Sigma) was added to the solution to enable subsequent cross-linking. Electrospinning was performed in the dark using a 20 G nozzle and 18 kV. The distance of the nozzle to the target collector was 15 cm. To induce crosslinks between the dimethacrylated groups, the initiator was activated with UV light (256 nm; 3J per side) subsequently after the electrospinning process. For the pure PLA scaffolds, 0.15 mg PLA was dissolved per mL HFP. The polymeric PLA-solution was then electrospun with a distance of 20 cm using 12 kV and an 18 G nozzle. Both scaffold types were treated with 70% ethanol and washed thoroughly with sterile cell culture water prior to cell seeding. Furthermore, the scaffold performance under physiological conditions was investigated [14]. Details are displayed in the [supplements](#).

2.2. Cell seeding and culture

Valvular endothelial cells (VECs) and valvular interstitial cells (VICs) were isolated from porcine heart valve leaflets by collagen digestion [15]. Endothelial cell growth medium (C-22010, Promocell, Heidelberg, Germany) was used for VECs and smooth muscle cell growth medium (C-22062, Promocell) was used for the culture of VICs. The medium was exchanged every second day. For cell–matrix interaction studies, 2.5×10^5 cells were seeded per PLA or PEGdma–PLA scaffold and cultured for 4 days at 37 °C and 5% CO₂. Cell viability was determined using an MTT assay.

2.3. Scanning electron microscopy (SEM)

Native tissues as well as unseeded and cell-seeded electrospun scaffolds were analyzed using a scanning electron microscope (1530 VP, Zeiss, Jena, Germany). All samples were rinsed with DPBS and incubated in a 2% glutaraldehyde solution for 45 min. To remove remaining water, the samples were passed through ascending alcohol concentrations (25%, 50%, 70%, 2 × 96% ethanol, isopropanol). Subsequently, the samples were dried at room temperature, mounted onto stubs and sputtered with platinum for 60 s.

2.4. Electron spectroscopy for chemical analysis (ESCA)

ESCA was performed to determine the atomic composition of the scaffold surfaces. Electrospun scaffolds were placed into the analysis chamber of the Axis Ultra device (Kratos Analytical, New York, USA) and a pressure of 10^{-9} mbar was applied. All samples were activated via X-rays and the kinetic energy of emitted auger and photoelectrons was measured. To validate the presence of both polymers (PEGdma and PLA) on the fiber surface, the obtained results were compared with known values from the literature for the single components.

2.5. Atomic force microscopy

Fresh dissected valve leaflets ($n = 4$) and electrospun scaffolds ($n = 3$) were immersed in water-soluble tissue freezing medium (14020108926, Leica, Nussloch, Germany) and immediately frozen at -80 °C. Cryosections with a thickness of 10–20 μm were prepared using a cryotome (Microm HM 560, Thermo Scientific, Waltham, MA, USA). The slides were thawed and brought to room temperature prior to AFM

measurements. A commercial AFM setup (MFP3D Bio, Asylum Research, Santa Barbara, CA) was used to perform force mapping [16] on the sample sections. The measurements were performed in phosphate buffered saline (PBS) using a single sphere-tip cantilever (FM-M-SPL, Nanoworld, Neuchâtel, Switzerland) [17] with a radius of 980 nm and a spring constant of 4.0 N/m, determined by the thermal noise of the cantilever [18]. Force–distance-curves were recorded within the scan area on 30×30 points (on the ventricularis, spongiosa and fibrosa layer of each leaflet) or on 40×40 points (on the scaffold sections). The scan area was chosen between $40 \times 40 \mu\text{m}^2$ and $90 \times 90 \mu\text{m}^2$, depending on the size of each layer. The force curve rate was 2.5 Hz, resulting in a force curve velocity of 20 μm/s. Each force–distance-curve was analyzed by fitting the spherical Hertz model [19], giving images of the local Young's modulus $\langle E \rangle$ as a dimension of local stiffness ("stiffness images").

For each stiffness image the layer-specific mean Young's modulus was calculated as the geometric mean, because the Young's modulus of tissues is log-normally distributed [20–22]. Statistical significance was determined by using Student's *t*-test on the logarithmic values. In addition, the mean moduli were averaged separately for each layer to give a total modulus $\langle E \rangle_{\text{total}}$ for each layer.

2.6. Uniaxial tensile testing

Native leaflets and electrospun scaffolds were cut into 10 mm × 40 mm rectangular pieces and clamped into the uniaxial tensile testing device (Zwick Roell, Ulm, Germany). The exact sample dimensions were determined before each measurement and recorded with the software for further calculations of Young's modulus, tensile strength and elongation. An initial load of 0.1 MPa was used and the scaffolds were then stretched with a velocity of 5 mm/min. Native leaflets were directly measured after dissection. For better comparison, the scaffolds were also measured in wet state. All measurements were performed at room temperature.

2.7. Contact angle measurement

Hydrophilicity of the electrospun substrates was analyzed with an OCA 40 (DataPhysics Instruments GmbH, Filderstadt, Germany). A water drop with the volume of 2 μl was placed onto the sample and the contact angle was measured using a video setup and the SCA20 software (DataPhysics Instruments).

2.8. Swelling ratio

To determine the water-holding capacity of the native valve tissues and electrospun scaffolds, the samples were weighed in their dry (W_{dry}) and wet state (W_{wet}) after 4 h swelling in water. The swelling ratio was calculated with the following formula:

$$\text{Swelling ratio}[\%] = \frac{W_{\text{wet}} - W_{\text{dry}}}{W_{\text{dry}}} \times 100$$

2.9. Immunofluorescence staining

Four days after VIC and VEC seeding, the scaffolds were rinsed with PBS and processed for antibody staining. Unspecific binding sites were blocked using goat serum. Paraffin-embedded human tissues were treated as previously described [23]. As primary antibodies served: anti-vWF (1:200; A0082, Dako, Hamburg, Germany), anti-αSMA (1:500; A2547, Sigma), anti-FAK (1:100; ab4803, Abcam, Cambridge, UK), anti-vinculin (1:500; MAB3574, Millipore, Darmstadt, Germany), anti-collagen type I (1:100; HPA008405, Sigma) and anti-versican (1:375; HPA004726, Sigma). After overnight incubation at 4 °C, the antibody solution was removed and the scaffolds were carefully rinsed with PBS. A fluorescence-conjugated secondary antibody (1:250; Alexa Fluor® 488, Molecular Probes, Darmstadt, Germany) served to visualize the protein. Alexa Fluor 546-conjugated phalloidin (1:50; A12381, Alexa Fluor® 546, Molecular Probes, Darmstadt, Germany) was added to the secondary antibody solution and the mixture was incubated for 25 min in the dark. Further washing steps followed prior to DAPI staining. Images were taken with a Laser Scanning Microscope (LSM710 inverted confocal microscope, Carl Zeiss, Jena, Germany).

2.10. Generation of a bio-functionalized leaflet

Electrospinning of PEGdma-PLA was performed as described earlier. A copper negative mold of a valve served as the collector (Suppl. Fig. 1). After electrospinning, the valve was removed from the mold and a collagen type I gel-coating was performed to mimic the fibrosa. For gel formation, a ratio of 2:1 collagen type I (10 mg/mL in acetic acid) and neutralization buffer was mixed and subsequently added onto the scaffold [24]. The construct was placed in an oven and dried at 60 °C for approximately 1 h. Furthermore, 50 μL human versican (H00001462-P01, Novus Biologicals, Littleton, USA) was mixed in PBS, containing 15% PEGdma and 0.01% photoinitiator. The tips of the leaflets were dipped in a versican–PEGdma solution and additionally crosslinked using 365 nm UV light in order to mimic the thick versican-containing tips of native heart valve leaflets. After fixation using 4% paraformaldehyde and paraffin embedding, 10 μm sections were generated and Alcian blue (visualization of PGs and GAGs) as well as Safranin (visualization of collagen-containing structures) staining were performed to visualize the engineered constructs and to compare it to native tissues.

2.11. Statistical analyses

Data are presented as mean \pm standard deviation unless stated otherwise. Statistical significance was determined by ANOVA using Origin software (OriginPro 8G, Northampton, UK). *p*-Values less than 0.05 were defined as statistically significant, unless stated otherwise.

3. Results

3.1. Scaffold characterization

Uniaxial tensile testing, SEM and swelling ratio calculations were utilized to characterize excised aortic heart valve leaflets and compare them to the electrospun scaffolds. The native fibrous leaflets were soft with a high (90%) water uptake capacity (Table 1). PLA is an elastic and electrospinnable polymer, which is used in clinics. Comparing the mechanical properties of native leaflets to those of electrospun PLA (Table 1), no significant differences were observable in regards to the Young's modulus (native: 62.4 ± 36.7 MPa; PLA: 64.1 ± 6.5 MPa; $p = 0.09$). However, PLA scaffolds showed a significantly higher expansibility (native: $5.5 \pm 3.0\%$; PLA: $275 \pm 37\%$; $p = 5.7 \times 10^{-8}$), and exhibited larger fiber diameters (native: 0.16 ± 0.06 μm ; PLA: 5.02 ± 1.10 μm ; $p = 1.4 \times 10^{-46}$) and pore sizes (native: 1.58 ± 1.42 μm^2 ; PLA: 1836 ± 1309 μm^2 ; $p = 1.3 \times 10^{-12}$). Additionally, PLA scaffolds were highly hydrophobic (contact angle: $131.8 \pm 2.8^\circ$) and could only store $11 \pm 9\%$ of water. PEGdma is a hydrophilic material with a high water uptake capacity. Therefore, we utilized PEGdma and fabricated PEGdma–PLA hybrid scaffolds in order to increase the water uptake capacity. Employing a half/half mixture of PEGdma and PLA led to an electrospinnable solution with photocrosslinkable fibers. Higher PEGdma concentrations were not spinnable, whereas lower concentrations could neither be crosslinked nor showed a more hydrophilic property (data not shown). The PEGdma–PLA hybrid scaffolds were highly hydrophilic (contact angle: $38.7 \pm 10.9^\circ$) and could absorb five times more water than PLA alone (PLA: $11 \pm 9\%$; PEGdma–PLA: $59 \pm 6\%$; $p = 7.5 \times 10^{-5}$). The contact angle was measured in the first second after water drop deposition. After 10 s, the water drop placed on the PEGdma–PLA scaffolds completely spread, indicating a high wettability. Despite the strong hydrophilicity, we could demonstrate with ESCA the presence of PEGdma and PLA domains facing the outside of the hybrid fibers (Suppl. Table 1). The combination of the two materials allowed a more natural material expansion (PLA: $275 \pm 37\%$; PEGdma–PLA: $4 \pm 0.4\%$), comparable to native leaflets ($5.5 \pm 3.0\%$), while not impacting the tensile strength (PLA: 2.0 ± 0.15 MPa; PEGdma–PLA: 2.1 ± 0.3 MPa). However, there was a significant increase of the Young's modulus when comparing PLA alone to PEGdma–PLA (64.1 ± 6.5 MPa versus 141 ± 23.6 MPa; $p = 0.006$).

Table 1
Mechanical properties of native heart valve leaflets and electrospun hybrid scaffolds.

	Native porcine leaflet	PLA	PEGdma–PLA
	<i>SEM</i>		
Fiber diameter (μm)	0.16 ± 0.06	5.02 ± 1.10^a	0.37 ± 0.08^b
Pore size (μm^2)	1.58 ± 1.42	1836 ± 1309^a	8.27 ± 6.23^b
	<i>Uniaxial tension</i>		
Young's modulus (MPa)	62.4 ± 36.7	64.1 ± 6.5	$141 \pm 23.6^{a,b}$
Tensile strength (MPa)	2.5 ± 0.9	2.0 ± 0.15	2.1 ± 0.3
Expansion in %	5.5 ± 3.0	275 ± 37^a	4 ± 0.4^b
Swelling ratio in %	90 ± 0	11 ± 9^a	$59 \pm 6^{a,b}$
Contact angle ($^\circ$)	–	131.8 ± 2.8	38.7 ± 10.9^b

^a Significant compared to native.

^b Significant compared to PLA.

SEM was performed for morphological assessments. When compared to the native leaflets (Fig. 1A), electrospun PLA scaffolds exhibited straight, randomly oriented fibers (Fig. 1B). Crosslinked PEGdma–PLA scaffolds were morphologically more similar to native leaflets (Fig. 1C). Additionally, a significant reduction of fiber and pore size could be achieved in the hybrid scaffolds. The fiber diameter (PLA: 5.02 ± 1.10 μm ; PEGdma–PLA: 0.37 ± 0.08 μm) and the pore size (PLA: 1836 ± 1309 μm^2 ; PEGdma–PLA: 8.27 ± 6.23 μm^2) of PEGdma–PLA were more comparable to native leaflets (fiber: 0.16 ± 0.06 μm ; pore: 1.58 ± 1.42 μm^2) (Table 1).

To assess the suitability of the PEGdma–PLA crosslinked scaffolds to serve as valve leaflets, we replaced a native leaflet of a porcine heart valve with the hybrid scaffold and simulated the in vivo situation in a bioreactor [14]. The PEGdma–PLA leaflet opened and closed properly and appeared to function well with the two remaining native leaflets (Suppl. Movie 1).

Supplementary video related to this article can be found at <http://dx.doi.org/10.1016/j.biomaterials.2013.10.080>.

3.2. AFM characterization

The native outflow tract valve leaflet is a three-layered tissue (Fig. 2A). AFM was employed to determine the Young's modulus of each individual layer (fibrosa, spongiosa and ventricularis) of a native heart valve leaflet (Fig. 2B) and the electrospun PEGdma–PLA scaffold (Fig. 2C). AFM force mapping was used to generate topography (Fig. 2D–G) and stiffness images (Fig. 2H–K) of both, heart valve leaflet and scaffold sections. Darker colors in the stiffness images indicate a lower local Young's modulus. In each measured porcine valve leaflet (Fig. 2L), the fibrosa and ventricularis layers were significantly stiffer when compared to the GAG-containing spongiosa ($p < 0.001$). As expected, the collagen-rich fibrosa layers were significantly stiffer when compared to the elastin-rich ventricularis layers ($p < 0.05$). The absolute values of the moduli, however, varied between leaflets, reflecting biological variability. We used the same method to determine the Young's modulus of the PEGdma–PLA hybrid scaffolds (Fig. 2M). The measured scaffold sections ($\langle E \rangle_{\text{total}} = 122 \pm 19$ kPa) were about $10\times$ stiffer when compared to the ventricularis ($\langle E \rangle_{\text{total}} = 12.3 \pm 4.6$ kPa) or the fibrosa ($\langle E \rangle_{\text{total}} = 13.8 \pm 5.0$ kPa) and about $20\times$ stiffer when compared to the spongiosa ($\langle E \rangle_{\text{total}} = 6.1 \pm 1$ kPa) of the porcine heart valve leaflets.

3.3. Cell-scaffold interactions

To determine cell–scaffold interactions as well as to exclude cytotoxic effects of the electrospun material, we seeded primary isolated VECs and VICs onto the PLA and PEGdma–PLA scaffolds. SEM images revealed that the cells adhered and spread on both scaffolds (Fig. 3). As revealed using an MTT assay, the cells on the scaffolds were able to metabolize the tetrazolium dye, indicating cytocompatibility of the electrospun materials (Suppl. Fig. 2). Four days after cell seeding, immunostaining was performed in order to identify potential cell phenotype changes and to demonstrate cell attachment (Fig. 4). The adhesion markers vinculin (Fig. 4C, D, K, L) and FAK (Fig. 4E, F, M, N) were both expressed in VECs and VICs cultured on PLA as well as on PEGdma–PLA scaffolds. FAK expression was significantly higher on PEGdma–PLA scaffolds (GVI per cell on PLA: 0.53 ± 0.04 ; PEGdma–PLA: 0.76 ± 0.03 ; $p = 8 \times 10^{-5}$). It could be further observed that there were fewer VECs on the PLA scaffolds when compared to the PEGdma–PLA scaffolds, a phenomenon that was not observed for VIC cultures in which the same confluence was achieved on both scaffolds. The actin cytoskeleton of VECs and VICs was much more distinct on the PEGdma–PLA matrices (Fig. 4A, B, I, J). Both VECs and VICs,

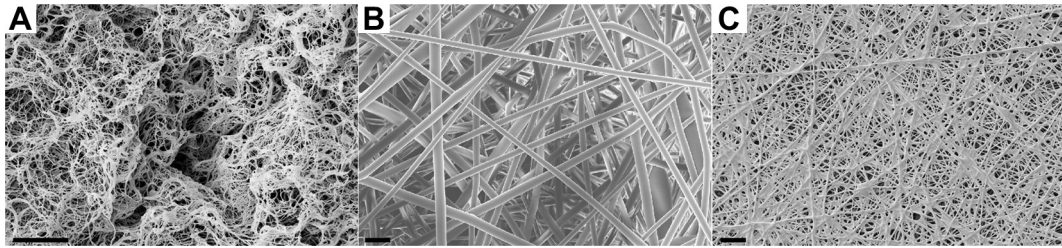


Fig. 1. SEM images of (A) a native heart valve leaflet, (B) electrospun PLA and (C) electrospun, UV-crosslinked PEGdma–PLA scaffolds. Scale bars equal 10 μm.

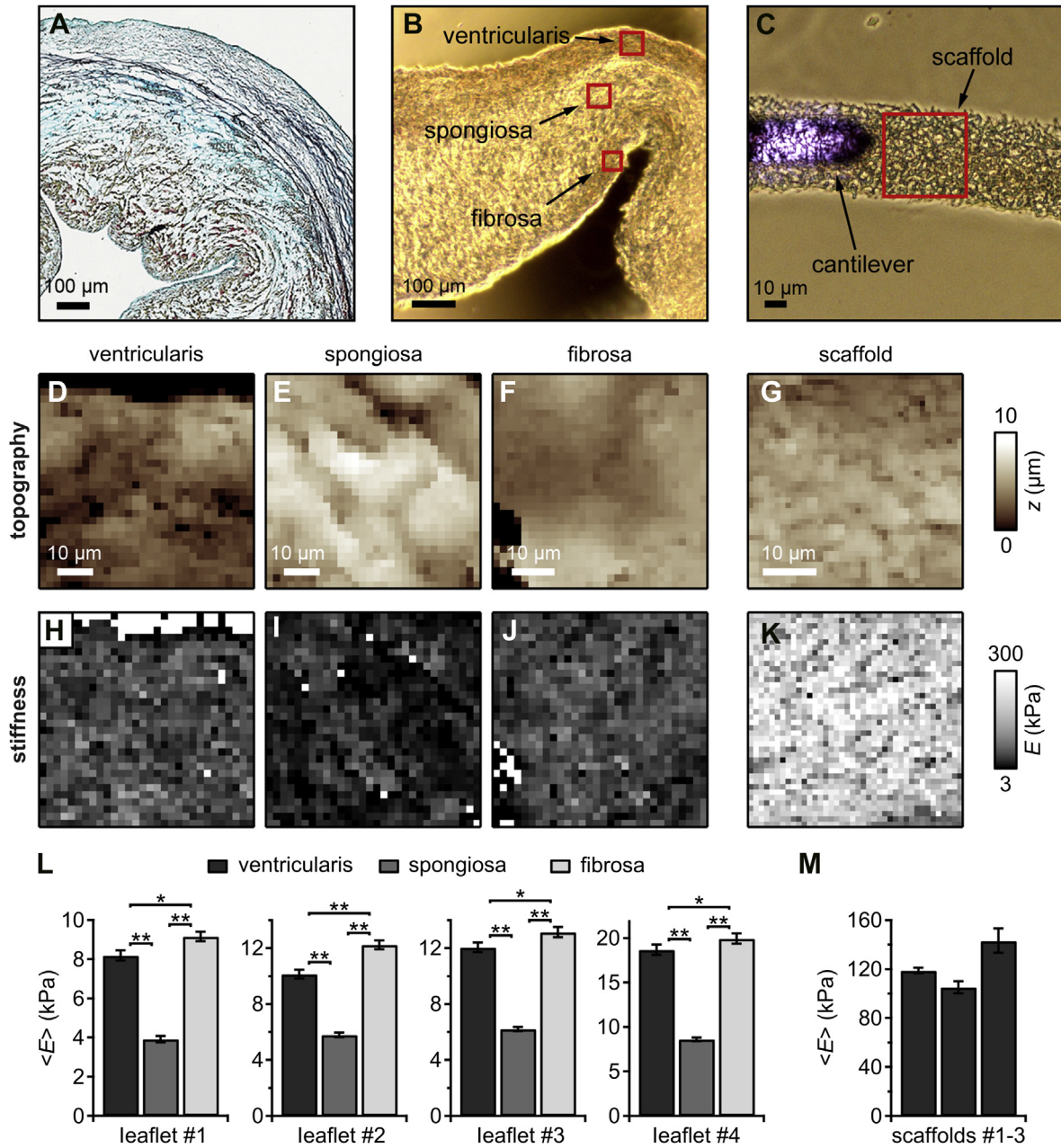


Fig. 2. AFM mapping on cryosections of porcine heart valve leaflets and PEGdma–PLA scaffolds: (A) Movat pentachrome staining of a native human heart valve leaflet. Elastic fibers in the ventricularis are black, the collagen-rich fibrosa is yellow, GAGs – mainly in the spongiosa – are stained blue and cell nuclei are shown in red/black. (B) Image of a porcine leaflet section with the AFM scan areas (red boxes) on the ventricularis, the spongiosa and the fibrosa. (C) Bright-field image of a PEGdma–PLA scaffold section with the AFM scan area (red box). (D–F) Topography images of a heart valve leaflet section. (G) Topography image of the PEGdma–PLA scaffold section. (H–K) Stiffness images correspond to the topography images (D–G). Darker colors indicate a lower local Young’s modulus. Layer-specific mean Young’s moduli (\pm standard error of the mean) are displayed for (L) the ventricularis, spongiosa and fibrosa layers of the porcine heart valves and (M) the electrospun PEGdma–PLA scaffold. * $p < 0.05$ and ** $p < 0.001$ indicate statistically significant differences using Student’s *t*-test.

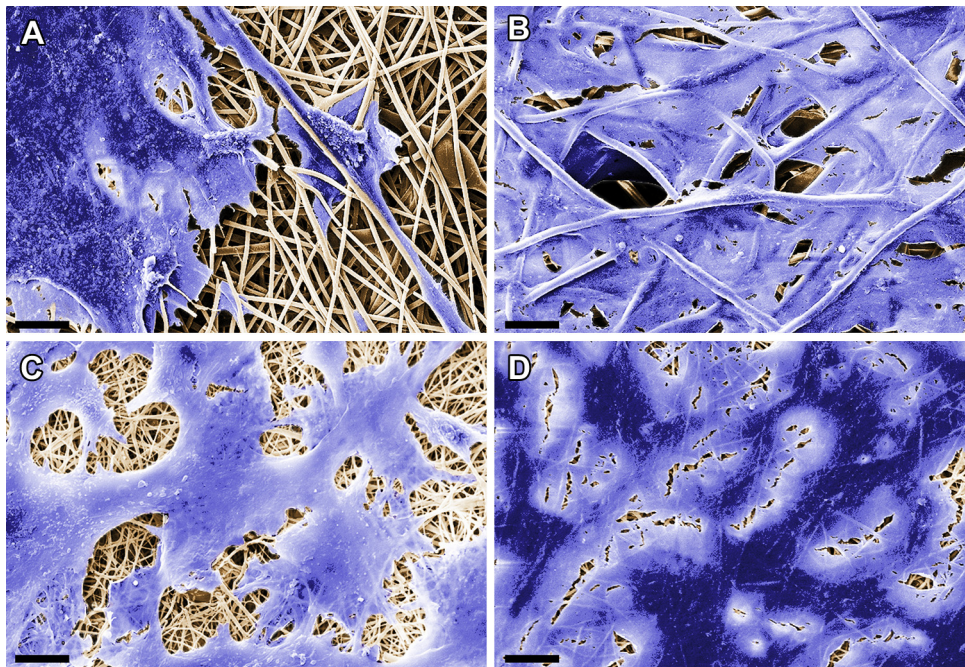


Fig. 3. SEM of cell-seeded electrospun scaffolds: (A) VICs on PLA, (B) VECs on PLA, (C) VICs on PEGdma–PLA and (D) VECs on PEGdma–PLA. Scale bars equal 15 μ m.

maintained their phenotype on PLA and PEGdma–PLA scaffolds (Fig. 4G, H, O, P).

3.4. Biofunctionalization – proof of principle

In order to identify crucial proteins that can be utilized for the functionalization of the PEGdma–PLA hybrid scaffolds, we studied early human heart valve development (Fig. 5). Although it had been previously reported that the cardiac jelly and early cardiac cushions are mainly composed of PGs, we revealed that collagen type I was also expressed at the onset of cushion formation in semilunar valves (Fig. 5A). Collagen type I protein expression remained present in all fetal (Fig. 5A, C, E) and postnatal leaflets (Suppl. Fig. 3A). Moreover, collagen type I expression was more distinctly found in the fibrosa as early as in the second trimester (Fig. 5E). Versican was highly expressed in the cushion mesenchyme of 3–4 week atria-ventricular valves (AVVs) and in the outflow tract (OFT) (Suppl. Fig. 3B). It was homogeneously expressed throughout the semilunar cushions and leaflets during the first trimester (Fig. 5B, D). The spatial distribution within the leaflet changed during the second trimester, where versican was more distinctly expressed close to the arterial wall and in the leaflet tip (Fig. 5F; white arrows). This expression pattern was maintained in the adolescent leaflet (Suppl. Fig. 3C–E). Alcian blue staining confirmed these expression patterns, with PGs predominantly expressed in the leaflet tip (Fig. 6A; blue), and collagen type I being present in the fibrosa layer (Fig. 6B; yellow). To closer mimic this valvular histoarchitecture, we modified in a proof-of-principle experiment the PEGdma–PLA scaffolds by introducing a versican-containing tip (Fig. 6C) and a collagen type I-composed gel layer (Fig. 6D).

4. Discussion

PLA is a degradable, aliphatic polyester, which is synthesized either by condensation polymerization of the free acid or by catalytic ring-opening polymerization of the lactide [25,26]. Due to its biocompatibility, it is a standard polymer in the biomedical field and is already used in clinics for drug delivery systems as well as for

sutures [25]. It has previously been shown that PLA has good mechanical properties with a Young's modulus of 3500 MPa and a tensile strength of 50 MPa [27]; however, these results refer to the bulk material. For electrospun PLA, we assessed in this study a Young's modulus of 64.1 MPa, which is comparable to results found in a previous study [28]. This modulus is similar to the Young's modulus of the native valve with 62.4 MPa; however, we aimed to find a material that mimics the multifactorial properties of the ECM and not only the Young's modulus. We identified that electrospun PEGdma–PLA in a ratio 1:1 possessed properties including pore sizes, fiber diameters, tensile strength and expansion similar to these seen in native valve leaflets. PEGdma–PLA scaffolds showed a significant lower water uptake capacity compared to the native valve; however, comparing the two polymer scaffolds, the PEGdma–PLA mixture had a significantly higher swelling ratio.

PLA is highly hydrophobic. We determined contact angles ranging between 129.3° and 135.6°, similar to what had been reported before (135.7° [28]). In order to prevent protein adsorption, it is necessary to lower the contact angle and modify the material to a more hydrophilic state. Biomaterials often fail in vivo due to inflammatory reactions. Thereby, proteins such as IgG and fibrinogen attach to the implant, leading to subsequent leukocyte adhesion and finally mediating a foreign body reaction [29]. This process is called "biofouling" and can be prevented by using hydrophilic surfaces. Several chemical groups have been identified to lower protein adsorption such as polyethylene glycol (PEG) [29,30]. Here, we aimed to combine the advantageous mechanical properties of PLA and the hydrophilic non-fouling characteristics of PEG. There are many ways to modify PEG such as linking selected proteins directly to the polymer [31]. Besides pharmaceutical applications, PEG is commonly used as a plasticizer for brittle polymers [32]. Jacobsen et al. had previously shown that the addition of PEG to PLA results in a decreased Young's modulus, a decreased tensile strength and a shorter elongation [27]. Here, we aimed to keep the stress–strain behavior and lower the elongation of PLA. PEGdma, which can be photochemically cross-linked, was used to additionally stabilize the fibrous scaffold. With an electrospun 1:1 mixture of PEGdma and PLA, we obtained a

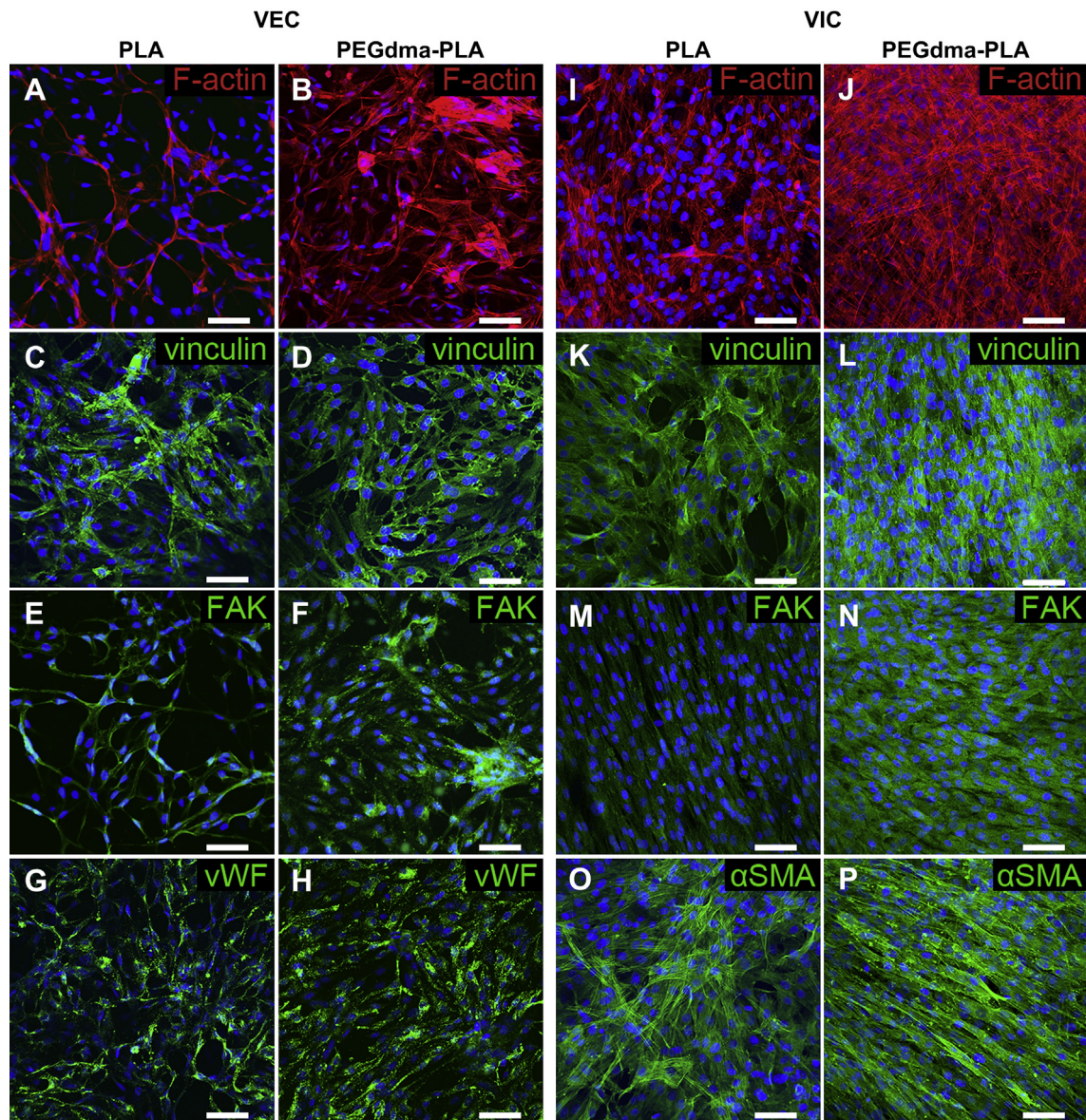


Fig. 4. Immunofluorescence staining of VEC- and VIC-seeded electrospun PLA and PEGdma-PLA scaffolds. Cell nuclei are depicted in blue (DAPI). Scale bars equal 50 μm .

material with the same tensile strength as PLA alone and as the native leaflet. Additionally, we could reduce the expansion of the material to the same value in vivo. In contrast to other studies [28], we found a significant higher Young's modulus of the PEGdma-PLA scaffold compared to PLA. However, Wang et al. [28] used a PEG content of only 30%. It has previously been shown that the Young's modulus decreases with increasing PEG concentration. As soon as the PEG content exceeds 30%, the Young's modulus increases [25]. We hypothesize that the high PEG content of 50% as well as the induced crosslinks of the methacrylated groups are responsible for the significant increase of the Young's modulus. Technically, it was only possible to measure the native leaflets in the direction of the collagen bundles due to their small size. It has been shown before, that the direction in which a leaflet is measured can impact the Young's modulus significantly [33,34]. However, in these studies it had not been considered that the native heart valve leaflets are three-layered heterogeneous tissues with mainly stiff collagen fibrils in the fibrosa and highly

extensible elastin with low stiffness in the ventricularis [35,36]. To obtain more detailed insights into the mechanics of the three individual layers, we applied AFM. We identified that the measured Young's modulus of the separate layers is much smaller than the modulus measured via uniaxial tensile tests. The AFM measurements are based on indentation of materials on the nanometer scale and the Young's moduli gained from these experiments represent the behavior of tissues on very small deformations. Different techniques such as uni or biaxial experiments might lead to different values regarding the stress-strain behavior of tissues on a much larger scale. In this study we determined that the fibrosa was stiffer than the ventricularis, which has already been shown by employing micropipette aspiration experiments [37]. However, with the AFM technique it was also possible to determine the Young's modulus of the spongiosa layer. Stradins et al. previously demonstrated that the mechanical properties of aortic and pulmonary valves are non-linear and significantly differ in circumferential and radial directions [34]. It has to be further

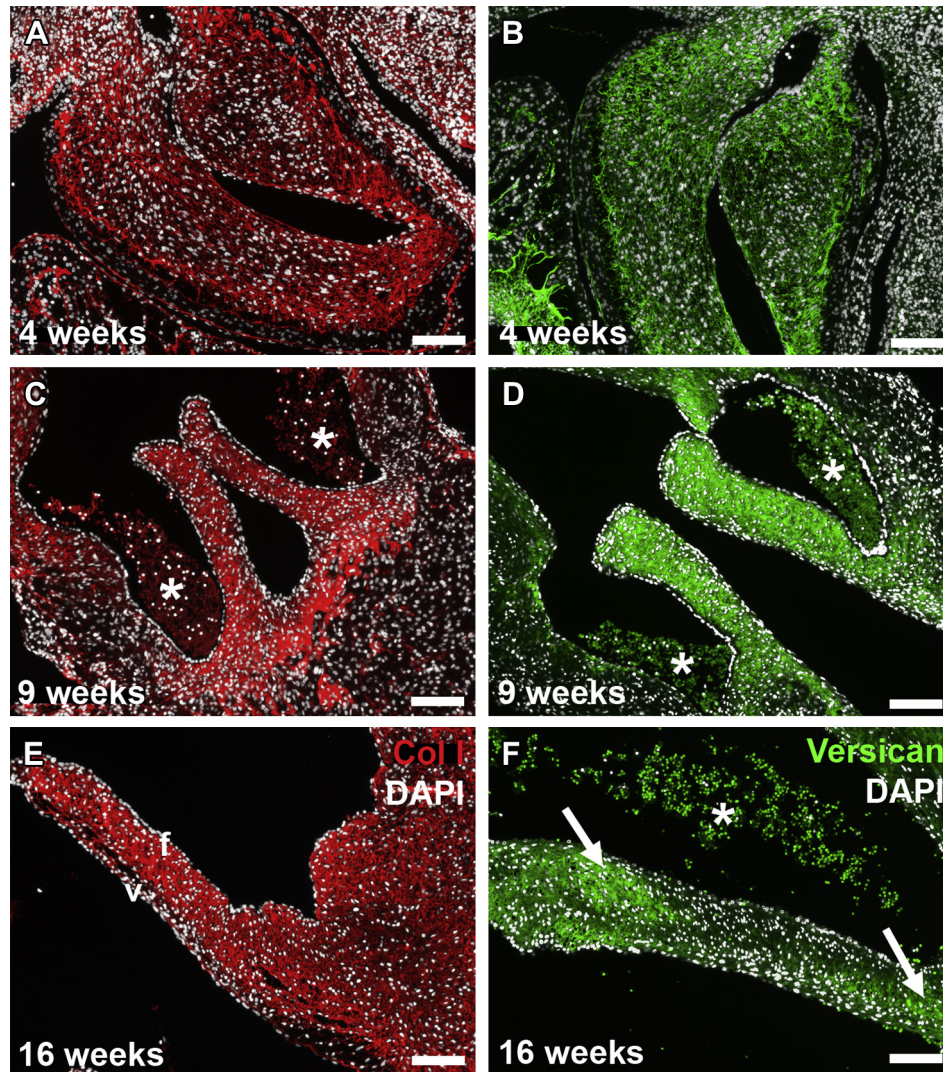


Fig. 5. Immunohistological analyses reveal protein expression patterns in developing human heart tissues. (A), (C), (E): collagen type I (red); (B), (D), (F): versican (green). Asterisks indicate erythrocytes. Scale bars equal 50 μm . fibrosa (f); ventricularis (v).

investigated whether this anisotropic behavior also affects the Young's modulus measured via AFM.

The use of the PEGdma–PLA hybrid material resulted in a scaffold with a fiber and pore size similar to native leaflets. A significant decrease of fiber and pore sizes by 30% due to PEG addition has been previously described [28]. Due to earlier reports that the fiber dimensions have an impact on cell viability and cell proliferation [38], it was important to adjust the fiber size and morphology towards these of native heart valve leaflets. Although the water uptake capacity of the PEGdma–PLA scaffolds still differed from the one of native leaflets, it was much better than the uptake seen in PLA scaffolds. Further improvements of the material by modifications such as GAG-coupling may achieve more physiological features.

It has been previously shown that electrospun 3D nano-fibrillar scaffolds with a high surface area-to-volume ratio can improve cell attachment and proliferation [39]. Here, we seeded primary isolated valvular cells onto pure PLA scaffolds and PEGdma–PLA hybrid scaffolds in order to study cell–scaffold interactions as well as cytotoxicity. vWF was used to confirm the VEC phenotype and αSMA , a marker that has been previously employed to characterize cultured VICs [40], was used to verify proliferative VICs. VECs

proliferated better on PEGdma–PLA scaffolds, whereas VICs behaved the same on either scaffold. These results are contrary to other studies, where cells showed a delayed adhesion and proliferation on hydrophilic PEG–substrates [28]. We speculate that the cells adhered on the hydrophilic scaffolds, where they were able to improve their proliferative capacity, which is in contrast to cultures on PLA substrates. Hence, despite the delayed cell adhesion, there are more VECs present. The increased cell proliferation of PEGdma–PLA scaffolds is based on the similarity to the native ECM. Additionally, a higher FAK expression could be determined for PEGdma–PLA scaffolds, indicating an increased cell proliferation due to the fact that FAK plays a crucial role in cell adhesion, proliferation, migration and cell survival [41]. Both immunofluorescence staining and scanning electron microscopy revealed well adhered, spread, phenotype-maintaining and, most important, viable cells on the generated PEGdma–PLA material indicating a good biocompatibility.

The generated PEGdma–PLA hybrid fiber scaffold is a promising base material for the generation of an engineered heart valve due to its superior structural and mechanical properties; however, further modifications have to be made to closer mimic the native tissue. Biofunctionalization of the base material using native proteins that

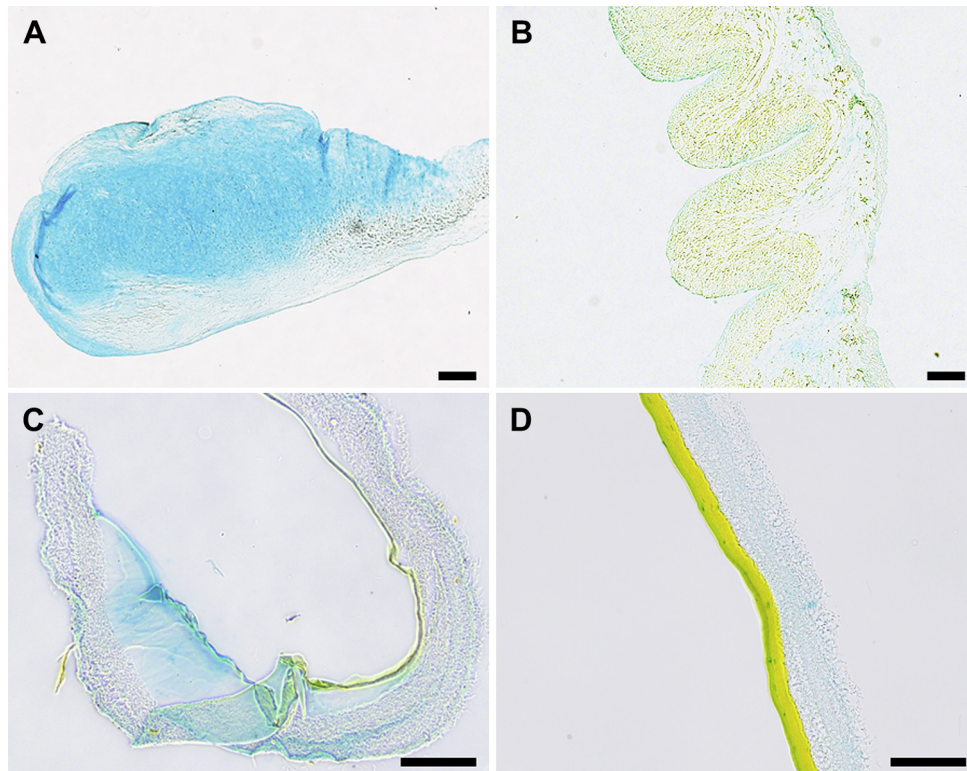


Fig. 6. Alcian blue and saffron staining of (A, B) a native 19 year old human aortic valve and (C, D) a tissue-engineered valve leaflet. Collagen is stained in yellow and proteoglycans are visualized in blue. Scale bar equals 200 μm .

are routinely expressed in native valve tissues such as GAGs or PGs could prove to be useful when aiming to lower for example the stiffness of the constructs. Highly negatively charged GAG-chains produce a hydrated gel-like structure [36]. In further studies, this phenomenon could be transferred to the scaffold by either applying simple coating techniques or even directly electrospin GAGs. Our group has previously reported that GAGs can be electrospun without the loss of function [5]. Tissue engineering is a technology that aims to mimic tissue and organ development. It is known, that collagen type I is responsible for stability and stiffness of many tissues and organs [42], whereas GAGs and PGs have been identified to maintain the water content [43]. In this study, we monitored ECM protein expression patterns during human semilunar valvulogenesis. Based on routine histological analyses, cardiac cushions consist only of PGs [44]. However, our data revealed that the structural protein collagen type I and versican were present in the early cardiac cushion mesenchyme, which differs from reports using human third trimester tissues [44] and AVV mouse embryonic tissues at E12.5, which equals the fifth week of human gestation [45]. The early and distinct collagen type I expression indicates that this structural protein is crucial for the human semilunar valve formation. During second trimester, collagen type I was predominantly detected in the fibrosa. These data demonstrate that a bilaminar ECM structure is already arranged by cells during this early developmental stage. Here, we identified that the stratification of human semilunar leaflets begins at the end of the first trimester, which is much earlier than previously projected [44,46]. Versican has been recognized as one of the earliest expressed PGs in the cardiac jelly of mice and is thought to be involved in endothelial–mesenchymal transition (EndMT) processes [47–49]. During EndMT, versican is thought to regulate the transition from highly proliferative endocardial cells to less proliferative remodeling

mesenchymal cells [50–53]. Our findings demonstrate that versican is similar to the rodent system expressed during early valvulogenesis. Versican was strongly detected throughout the cardiac cushions and rudimentary leaflets. Therefore, we hypothesize that versican is a key regulator of valvulogenesis as it facilitates EndMT and neural crest-derived cell migration [53,54], which are both crucial events during early cardiac cushion formation and leaflet elongation. The spatial distribution of versican changes within the second trimester. Here, versican was predominately found at the annulus and tip of the leaflet. This remarkable distribution pattern points out the importance of collagen type I and versican. In order to generate an off-the-shelf heart valve with growth potential, it is necessary that the PEGdma–PLA base material enables further modifications. Technically, it was possible to achieve the two-layered structure as well as the PG tip; however, while embedding and sectioning, the versican tip lost its original shape.

5. Conclusion

In this study, we identified the mechanical properties of native outflow tract valve leaflets in order to translate our findings in the design of a suitable biomaterial for the application in heart valve tissue engineering. We established a method to determine the Young's modulus of the three individual leaflet layers. Employing AFM enabled a valuable first insight into the spongiosas' mechanical properties. Moreover, we generated PEGdma–PLA hybrid scaffolds via electrospinning, which showed biomechanical properties that resembled the native valve matrix. Cell seeding experiments confirmed viable and phenotype-maintaining valvular cells, concluding that the hybrid material possessed no cytotoxic properties. Moreover, we biochemically modified the hybrid scaffolds utilizing ECM proteins that have been identified to play a crucial

role in human heart valve development. Therefore, the generated scaffolds are a promising material for the production of a potentially human-based off-the-shelf heart valve.

Acknowledgments

We thank Pirmin Lakner and Simone Liebscher (both University Women's Hospital Tübingen, Germany), Daniel A. Carvajal Berrio, Christian Becker and Daniel Özdemir (Fraunhofer IGB Stuttgart, Germany) for their technical support, and Shannon Lee Layland (Fraunhofer IGB Stuttgart, Germany) for his appreciated comments on the manuscript. We also thank Ulrich A. Stock (University Hospital Frankfurt, Germany) for the access to the valve bioreactor system. The authors are grateful for the financial support by the Fraunhofer-Gesellschaft Internal programs (Attract 692263 to KSL), the BMBF (0316059 to KSL) and the Ministry of Science, Research and the Arts of Baden-Württemberg (33-729.55-3/214 to KSL).

Appendix A. Supplementary data

Supplementary data related to this article can be found at <http://dx.doi.org/10.1016/j.biomaterials.2013.10.080>.

References

- [1] Sewell-Loftin MK, Chun Y, Khademhosseini A, Merryman WD. EMT-inducing biomaterials for heart valve engineering: taking cues from developmental biology. *J Cardiovasc Transl Res* 2011;4:658–71.
- [2] Frantz C, Stewart KM, Weaver VM. The extracellular matrix at a glance. *J Cell Sci* 2010;123:4195–200.
- [3] Agarwal S, Wendorff JH, Greiner A. Progress in the field of electrospinning for tissue engineering applications. *Adv Mater* 2009;21:3343–51.
- [4] Schenke-Layland K, Xie J, Angelis E, Starcher B, Wu K, Riemann I, et al. Increased degradation of extracellular matrix structures of lacrimal glands implicated in the pathogenesis of Sjogren's syndrome. *Matrix Biol* 2008;27:53–66.
- [5] Hinderer S, Schesny M, Bayrak A, Ibold B, Hampel M, Walles T, et al. Engineering of fibrillar decorin matrices for a tissue-engineered trachea. *Biomaterials* 2012;33:5259–66.
- [6] Li M, Mondrinos MJ, Gandhi MR, Ko FK, Weiss AS, Lelkes PI. Electrospun protein fibers as matrices for tissue engineering. *Biomaterials* 2005;26:5999–6008.
- [7] Hopkins AM, De Laporte L, Tortelli F, Spedden E, Staii C, Atherton TJ, et al. Silk hydrogels as soft substrates for neural tissue engineering. *Adv Funct Mater* 2013. <http://dx.doi.org/10.1002/adfm.201300435>.
- [8] Kim TG, Shin H, Lim DW. Biomimetic scaffolds for tissue engineering. *Adv Funct Mater* 2012;22:2446–68.
- [9] Hanjaya-Putra D, Wong KT, Hirotsu K, Khetan S, Burdick JA, Gerecht S. Spatial control of cell-mediated degradation to regulate vasculogenesis and angiogenesis in hyaluronan hydrogels. *Biomaterials* 2012;33:6123–31.
- [10] Schenke-Layland K, Nsair A, Van Handel B, Angelis E, Gluck JM, Votteler M, et al. Recapitulation of the embryonic cardiovascular progenitor cell niche. *Biomaterials* 2011;32:2748–56.
- [11] Jacot JG, McCulloch AD, Omens JH. Substrate stiffness affects the functional maturation of neonatal rat ventricular myocytes. *Biophys J* 2008;95:3479–87.
- [12] Bronshtein T, Au-Yeung GCT, Sarig U, Nguyen EB-V, Mhaisalkar PS, Boey FYC, et al. A mathematical model for analyzing the elasticity, viscosity, and failure of soft tissue: comparison of native and decellularized porcine cardiac extracellular matrix for tissue engineering. *Tissue Eng Part C Methods* 2012;19:620–30.
- [13] Arjunon S, Rathana S, Jo H, Yoganathan A. Aortic valve: mechanical environment and mechanobiology. *Ann Biomed Eng* 2013;41:1331–46.
- [14] Schleicher M, Sammler G, Schmauder M, Fritze O, Huber A, Schenke-Layland K, et al. Simplified pulse reactor for real-time long-term in vitro testing of biological heart valves. *Ann Biomed Eng* 2010;38:1919–27.
- [15] Schenke-Layland K, Riemann I, Opitz F, König K, Halbhuber KJ, Stock UA. Comparative study of cellular and extracellular matrix composition of native and tissue engineered heart valves. *Matrix Biol* 2004;23:113–25.
- [16] Radmacher M, Fritz M, Kacher CM, Cleveland JP, Hansma PK. Measuring the viscoelastic properties of human platelets with the atomic force microscope. *Biophys J* 1996;70:556–67.
- [17] Braunsman C, Hammer CM, Rheinlaender J, Kruse FE, Schäffer TE, Schlötzer-Schrehardt U. Evaluation of lamina cribrosa and peripapillary sclera stiffness in pseudoexfoliation and normal eyes by atomic force microscopy. *Invest Ophthalmol Vis Sci* 2012;53:2960–7.
- [18] Cook SM, Schäffer TE, Chynoweth KM, Wigton M, Simmonds RW, Lang KM. Practical implementation of dynamic methods for measuring atomic force microscope cantilever spring constants. *Nanotechnology* 2006;17:2135.
- [19] Hertz H. Ueber die Berührung fester elastischer Körper. *J Reine Angew Math* 1882;156.
- [20] Cross SE, Jin Y-S, Rao J, Gimzewski JK. Nanomechanical analysis of cells from cancer patients. *Nat Nanotechnol* 2007;2:780–3.
- [21] Hayenga HN, Trache A, Trzeciakowski J, Humphrey JD. Regional atherosclerotic plaque properties in ApoE^{-/-} mice quantified by atomic force, immunofluorescence, and light microscopy. *J Vasc Res* 2011;48:495–504.
- [22] Shimizu Y, Kihara T, Haghparast SMA, Yuba S, Miyake J. Simple display system of mechanical properties of cells and their dispersion. *PLoS One* 2012;7:e34305.
- [23] Votteler M, Berrio DAC, Horke A, Sabatier L, Reinhardt DP, Nsair A, et al. Elastogenesis at the onset of human cardiac valve development. *Development* 2013;140:2345–53.
- [24] Pudlas M, Koch S, Bolwien C, Thude S, Jenne N, Hirth T, et al. Raman spectroscopy: a noninvasive analysis tool for the discrimination of human skin cells. *Tissue Eng Part C Methods* 2011;17:1027–40.
- [25] Sheth M, Kumar RA, Davé V, Gross RA, McCarthy SP. Biodegradable polymer blends of poly(lactic acid) and poly(ethylene glycol). *J Appl Polym Sci* 1997;66:1495–505.
- [26] Buchatip S, Petchsuk A, Kongsuwan K. Synthesis and mechanical properties of poly(LLA-co-DLLA) copolymers. *J Magn Magn Mater* 2008;18:175–80.
- [27] Jacobsen S, Fritz HG. Plasticizing polylactide—the effect of different plasticizers on the mechanical properties. *Polym Eng Sci* 1999;39:1303–10.
- [28] Wang B-Y, Fu S-Z, Ni P-Y, Peng J-R, Zheng L, Luo F, et al. Electrospun polylactide/poly(ethylene glycol) hybrid fibrous scaffolds for tissue engineering. *J Biomed Mater Res A* 2012;100A:441–9.
- [29] Bridges AW, Garcia AJ. Anti-inflammatory polymeric coatings for implantable biomaterials and devices. *J Diabetes Sci Technol* 2008;2:984–94.
- [30] Kim P, Kim DH, Kim B, Choi SK, Lee SH, Khademhosseini A, et al. Fabrication of nanostructures of polyethylene glycol for applications to protein adsorption and cell adhesion. *Nanotechnology* 2005;16:2420.
- [31] Roberts MJ, Bentley MD, Harris JM. Chemistry for peptide and protein PEGylation. *Adv Drug Deliv Rev* 2002;54:459–76.
- [32] Baiardo M, Frisoni G, Scandola M, Rimelen M, Lips D, Ruffieux K, et al. Thermal and mechanical properties of plasticized poly(L-lactide). *J Appl Polym Sci* 2003;90:1731–8.
- [33] Masoumi N, Johnson KL, Howell MC, Engelmayr Jr GC. Valvular interstitial cell seeded poly(glycerol sebacate) scaffolds: toward a biomimetic in vitro model for heart valve tissue engineering. *Acta Biomater* 2013;9:5974–88.
- [34] Stradins P, Laciis R, Ozolanta I, Purina B, Ose V, Feldmane L, et al. Comparison of biomechanical and structural properties between human aortic and pulmonary valve. *Eur J Cardiothorac Surg* 2004;26:634–9.
- [35] Chen Q, Bruyneel A, Carr C, Czernuszka J. Bio-mechanical properties of novel bi-layer collagen-elastin scaffolds for heart valve tissue engineering. *Procedia Eng* 2013;59:247–54.
- [36] Taylor PM, Cass AEG, Yacoub MH. Extracellular matrix scaffolds for tissue engineering heart valves. *Prog Pediatr Cardiol* 2006;21:219–25.
- [37] Zhao R, Sider KL, Simmons CA. Measurement of layer-specific mechanical properties in multilayered biomaterials by micropipette aspiration. *Acta Biomater* 2011;7:1220–7.
- [38] He L, Liao S, Quan D, Ma K, Chan C, Ramakrishna S, et al. Synergistic effects of electrospun PLLA fiber dimension and pattern on neonatal mouse cerebellum C17.2 stem cells. *Acta Biomater* 2010;6:2960–9.
- [39] Mo XM, Xu CY, Kotaki M, Ramakrishna S. Electrospun P(LLA-CL) nanofiber: a biomimetic extracellular matrix for smooth muscle cell and endothelial cell proliferation. *Biomaterials* 2004;25:1883–90.
- [40] Chester AH, Taylor PM. Molecular and functional characteristics of heart-valve interstitial cells. *Philos Trans R Soc B Biol Sci* 2007;362:1437–43.
- [41] Luo M, Guan J-L. Focal adhesion kinase: a prominent determinant in breast cancer initiation, progression and metastasis. *Cancer Lett* 2010;289:127–39.
- [42] Mecham RP. Overview of extracellular matrix. *Curr Protoc Cell Biol* 2001;10.1.1–10.1.14.
- [43] Schaefer L, Schaefer RM. Proteoglycans: from structural compounds to signaling molecules. *Cell Tissue Res* 2010;339:237–46.
- [44] Aikawa E, Whittaker P, Farber M, Mendelson K, Padera RF, Aikawa M, et al. Human semilunar cardiac valve remodeling by activated cells from fetus to adult: implications for postnatal adaptation, pathology, and tissue engineering. *Circulation* 2006;113:1344–52.
- [45] Peacock JD, Lu Y, Koch M, Kadler KE, Lincoln J. Temporal and spatial expression of collagens during murine atrioventricular heart valve development and maintenance. *Dev Dyn* 2008;237:3051–8.
- [46] Lindsey SE, Butcher JT. The cycle of form and function in cardiac valvulogenesis. *Global Cardiol Sci Pract* 2011;2011(2):10.
- [47] Schroeder J, Jackson L, Lee D, Camenisch T. Form and function of developing heart valves: coordination by extracellular matrix and growth factor signaling. *J Mol Med* 2003;81:392–403.
- [48] Kruithof BPT, Krawitz SA, Gaussen V. Atrioventricular valve development during late embryonic and postnatal stages involves condensation and extracellular matrix remodeling. *Dev Biol* 2007;302:208–17.
- [49] Henderson DJ, Copp AJ. Versican expression is associated with chamber specification, septation, and valvulogenesis in the developing mouse heart. *Circ Res* 1998;83:523–32.

- [50] Hinton RB, Lincoln J, Deutsch GH, Osinska H, Manning PB, Benson DW, et al. Extracellular matrix remodeling and organization in developing and diseased aortic valves. *Circ Res* 2006;98:1431–8.
- [51] Hatano S, Kimata K, Hiraiwa N, Kusakabe M, Isogai Z, Adachi E, et al. Versican/Pg-M is essential for ventricular septal formation subsequent to cardiac atrioventricular cushion development. *Glycobiology* 2012;22:1268–77.
- [52] Lincoln J, Alfieri CM, Yutzey KE. Development of heart valve leaflets and supporting apparatus in chicken and mouse embryos. *Dev Dyn* 2004;230:239–50.
- [53] Wight TN. Versican: a versatile extracellular matrix proteoglycan in cell biology. *Curr Opin Cell Biol* 2002;14:617–23.
- [54] Perissinotto D, Iacopetti P, Bellina I, Doliana R, Colombatti A, Pettway Z, et al. Avian neural crest cell migration is diversely regulated by the two major hyaluronan-binding proteoglycans PG-M/versican and aggrecan. *Development* 2000;127:2823–42.